AIAA JOURNAL
Vol. 30, No. 6, June 1992

Impact Response of Orthotropic Composite Plates Predicted from a One-Parameter Differential Equation

Robin Olsson*
FFA, Aeronautical Research Institute of Sweden, S-161 11 Bromma, Sweden

This paper presents an approximate analytical solution for the dynamic response of an infinite specially orthotropic plate impacted by an impactor with a semispherical tip. Thus, the solution is valid for low mass impacts. The analysis is an extension and rederivation of a solution for isotropic plates proposed by Zener. The analysis assumes a Hertzian contact law and is based on Kirchhoff's plate equation. The plate response is expressed in terms of contact force, contact pressure, central displacement, central curvature, and size of the impact affected area. The response is computed from a dimensionless differential equation in time, which is only dependent on the inelasticity parameter lambda. Lambda is a function of the impact velocity and variables describing the impactor and the plate. For a given lambda, the response can be interpolated from the solution plots for a number of representative values of lambda. Results computed from the model are compared with published numerical analyses and a number of experiments, and a close agreement is noted. Finally, the analysis shows the time-dependent velocity of a flexural wave propagating from the impact center.

Nomenclature

A = relation between flexural stiffnesses D_{ij}, Eq. (18)
a = length in x direction of wave-affected area (Fig. 2)
a_{ij} = a, related to a specific mode ij (Fig. 2)
b = length in y direction of wave-affected area (Fig. 2)
b_{ij} = b, related to a specific mode ij (Fig. 2)
c = radius of contact area (Fig. 1)
c_F = velocity of flexural waves, Eq. (42)
c_S = velocity of shear waves, Eq. (37)
D_{ij} = flexural stiffness
D^* = effective plate stiffness, Eq. (20)
E_c = apparent modulus of elasticity in contact stiffness, Eq. (5)
E_i = modulus of elasticity of object i
E_i' = apparent E_i, Eq. (4)
F = contact force, Eq. (2)
h = plate thickness (Fig. 1)
I = impulse transferred to the plate, Eq. (33)
j = mode number (number of half-waves) in x direction
k = mode number (number of half-waves) in y direction
k_c = contact stiffness, Eq. (3)
m = plate mass per unit area
p = contact pressure, Eq. (6)
R = impactor nose radius
r = radius from impact center (Fig. 1)
s = integration dummy variable
T = time constant, Eq. (29)
t = fixed time from beginning of impact
w_i = displacement of mass center of object i (Fig. 1)
W_{jk} = eigenfunction of mode jk of a simply supported plate, Eq. (10)
x, y = global in-plane plate coordinates (Fig. 2)
z = global out-of-plane plate coordinate
β = material constant in integration, Eq. (21)
δ = indentation, Eq. (1)
θ = in-plane angle from x axis
κ_i = plate curvature, Eq. (49)
λ = nondimensional impact parameter, Eq. (30)
ν_i = equivalent Poisson's ratio for transverse load on object i
ν_{ij} = Poisson's ratio for the plate and plies
ρ_i = density of object i
τ = variable time
ω_{jk} = angular frequency of mode jk, Eq. (17)

Indices

X_F = flexural value
X_{jk} = connected with mode jk
$X_{x,y,z}$ = X related to x,y,z
X_1 = X of the plate
X_2 = X of the impactor
X_{11} = X related to mode 1,1
X_{mn} = (m,n explicit numbers) X referring to local ply axes, m,n

I. Introduction

A WELL-KNOWN problem with laminated composite plates is their sensitivity to impact and the resulting damage, often in the form of invisible internal delaminations. The first step in understanding the causes and prevention of impact damage is a basic understanding of the dynamic impact response and how it is affected by different parameters. Ideally, closed-form solutions are desired for the response. However, the analytical treatment of impacts on plates faces considerable difficulties. These include the contact problem between impactor and plate, an almost point-like contact load, and a transient forced motion of the plate that is coupled to the contact problem. A complicating factor in composite plates is that shear deformations and bending-twisting coupling may have to be considered.

Impacts are often classified as "low velocity" and "high velocity" impacts. Tool dropping exemplifies low velocity impact, hail and runway stones high velocity impact.

From a phenomenological point of view, however, a more relevant classification would be impacts where the response is controlled by the boundary conditions and where it is controlled by wave propagation. In the boundary-controlled cases, the entire plate is deformed during the impact. When the contact time is much longer than the period of the lowest vibration mode, it could be termed as quasistatic, and the contact force and plate response are in phase. In the wave-controlled cases, the maximum contact force and plate response

Received Jan. 4, 1991; revision received Sept. 26, 1991; accepted for publication Oct. 1, 1991.

*Research Engineer, Structures Department, P. O. Box 11021.

are never in phase, and the plate deformation is localized to a region around the impact point. The kind of response is dependent on impactor velocity and mass as well as dimensions and properties of the plate. In a recent study,[1] low velocity impacts with small masses were used to produce responses that are normally termed as high velocity impacts. The damage resulting from these fundamentally different categories of impact has been studied experimentally by Cantwell and Morton.[2] The basic theory of impact is treated in Ref. 3.

The boundary-controlled quasistatic case has been analyzed by a considerable number of researchers[4-7] and by numerous experimenters.[6,8-10] Most experimental works do not make a distinction between boundary-controlled and wave-controlled impact response. Furthermore, they are usually limited to postimpact studies.

The boundary-controlled dynamic case of isotropic plates was treated by Karas in 1939.[11] The analyses of general dynamical impact response involving both wave propagation and boundary influence are limited to numerical studies that are either based on the finite element method[12-17] or on serial expansions of numerically computed eigenmodes.[18-21] A comparative study of these methods was given in Ref. 22. Recently, some analyses have been presented for impact on cylinders.[23,24]

The object of the present study was to increase the understanding of factors affecting the impact damage by finding a simple analytical solution for the impact response of composite plates.

The analysis is limited to the first impact phase where flexural waves have not yet been reflected from the boundaries. In all nonquasistatic cases encountered in the literature, maximum contact force occurs during this phase. A solution for nonshear deformable isotropic plates was given by Zener in 1941.[25] A more general solution for the transient forced motion of infinite isotropic plates was given by Sneddon in 1944.[26] Later, elements from Zener's and Sneddon's theories were used by Schweiger[27,28] to analyze impact experiments with isotropic plates. Recently, Mittal[29] presented a solution for shear deformable transversally isotropic plates. In the present paper, Zener's basic approach has been generalized to specially orthotropic plates. However, the derivation has been done in a more stringent way than originally. Furthermore, expressions have been derived for flexural strains and wave propagation. A more extensive description of the theory is given in Ref. 30, although the present paper includes improved expressions for flexural strains.

II. Contact Laws

In this study a Hertzian contact law has been used to describe the contact phenomenon. Hertz's theory was originally developed for a static load on an isotropic linear elastic halfspace, but it has been shown[3,31] to be a good approximation at moderate strain rates and highly local permanent deformation. A basic prerequisite in the impact on plates is also that the indentation depth is much smaller than the dimensions of both the contacting bodies and the contact area. For the case of a sphere against an isotropic plate (Fig. 1), Hertz's theory states that the indentation is

$$\delta = w_2 - w_1 \tag{1}$$

and the contact force is

$$F = k_c \delta^{3/2} \tag{2}$$

where

$$k_c = \frac{4}{3} E_c \sqrt{R} \tag{3}$$

with

$$E_i' = E_i/(1 - \nu_i^2) \tag{4}$$

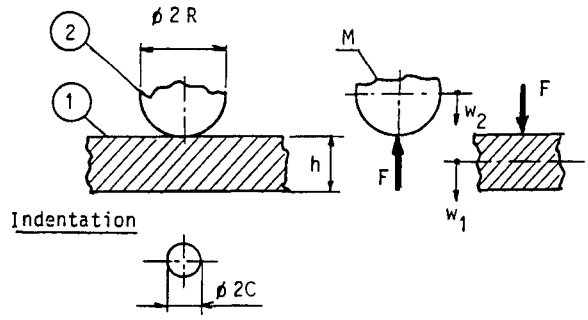

Fig. 1 Parameters in the contact problem.

and

$$1/E_c = 1/E_1' + 1/E_2' \tag{5}$$

For the case where the indentor is much stiffer than the target, Eq. (5) simplifies to $1/E_c \approx 1/E_1'$.

The contact pressure is

$$p(r) = \frac{3F}{2\pi c^2}\sqrt{1 - r^2/c^2}, \quad 0 \le r \le c \tag{6}$$

and the contact radius

$$c = \sqrt{R\delta} \tag{7}$$

For nonisotropic plates the material compliance $1/E_1'$ must be modified.

The logical extension of Eq. (4) for transversally isotropic plates is

$$E_1' = E_z/(1 - \nu_{rz}\nu_{zr}) \tag{8a}$$

In most laminated plates $\nu_{zr} \approx 0$, and the expression simplifies to

$$E_1' = E_z \tag{8b}$$

A more advanced expression for transversally isotropic materials has been derived by Conway and referred to by Greszczuk.[32]

In an orthotropic plate, the transversal compliance of Eq. (8a) becomes directionally dependent. It can be estimated by integrating over 2π and taking the average. However, since in most laminated plates $\nu_{zr} \approx 0$, the solution again simplifies to Eq. (8b). This brings $1/E_c$ into agreement with the expression proposed by S. H. Yang and C. T. Sun (compare with Ref. 12).

A more advanced closed expression is not known for generally orthotropic laminates, although a numerical solution by Greszczuk and Chao has been shown[32] to be relatively insensitive to in-plane fiber orientations. The indentation that is circular in transversally isotropic plates becomes elliptical in orthotropic plates. This effect is, however, very small. According to the numerical solution by Greszczuk and Chao, the axis ratio of the ellipse was only 1.07 for $E_{xx}/E_{yy} = 14.3$. According to experimental studies by Moon, referred to in Ref. 32, the indentation was only slightly elliptical for a unidirectional laminate.

On this basis, the following approximations seem highly justified for an orthotropic plate: 1) indentation is circular, and 2) transversal stiffness E_1' is given by Eq. (8a) or (8b). In the case of Eq. (8a), the properties should be the averaged in-plane properties.

For laminated composite plates, Tan and Sun[33] and others have experimentally found a good correlation with the Hertz 1.5 power law during quasistatic loading and less good during unloading. However, k_c was only determined as an empirical constant. The results were shown to be valid for dynamic

loads by comparison between an impact experiment and predictions from a finite element analysis based on the static loading/unloading laws.

In numerical solutions, it is common to set the transversal Young's modulus of the laminate equal to that of a ply, i.e., $E_z = E_{22}$. However, due to the constraints imposed by lamination, the transversal modulus of the laminate is larger than that of a single ply. This has been shown experimentally and theoretically by Henriksson,[34] who studied the special case of a cross-ply laminate where E_z was found to be $1.25 \cdot E_{22}$. This study also verified the contact law of Eq. (2) using stiffnesses of Eqs. (3), (4), (5), and (8b).

Using the transversal stiffness from Ref. 34 seems to considerably reduce the difference between theoretical contact moduli E_c and the ones obtained by Tan and Sun.

III. Derivation of Governing Equations

A basic assumption in the present analysis is that the time involved is so short that bending waves do not reflect from boundaries. In many impact cases, this assumption is highly justified as will be shown in Sec. V. It must, however, be pointed out that the model ceases to be valid as soon as such a reflection takes place.

The analysis is based on Kirchhoff's plate theory for specially orthotropic plates. The response of a plate can be expressed by time integration of the sum of modal impulse responses using orthogonal normalized eigenmodes.[35] For a plate with zero damping, the response in a point x, y to a point load in x_0, y_0 is given by

$$w_1(x,y,t) = \int_0^t F(\tau) \sum_{j=1}^{\infty} \sum_{k=1}^{\infty} \frac{W_{jk}(x,y) W_{jk}(x_0,y_0)}{m \omega_{jk}} \sin[\omega_{jk}(t-\tau)]\, d\tau \tag{9}$$

The neglect of damping is normally justified in short time impacts. The reasons are discussed in Ref. 30.

In an orthotropic plate, the flexural wave fronts scatter as almost elliptical rings centered in the impact point,[36] as sketched in Fig. 2a. We now approximate the area affected by impact with a simply supported rectangular plate with side lengths a and b as shown in Fig. 2b.

The normalized eigenfunctions of the plate are

$$W_{jk} = \frac{2}{\sqrt{ab}} \cos\frac{j\pi x}{a} \cos\frac{k\pi y}{b} \tag{10}$$

$$W_{jk} = 0 \text{ at } x = \pm a/2, \quad y = \pm b/2 \quad \text{implies } j,k = \text{odd} \tag{11}$$

The fact that the waves are closed ellipses implies

$$j \equiv k \tag{12}$$

The assumption $j = k$ implies that the ratio a/b is equal to the ratio of wavelengths. These are the inverses of the wave numbers $k_i = \omega_{jk}/C_{Fi}$ $(i = x,y)$. Assuming the flexural wave velocities C_{Fi} to be given by Eq. (36), we obtain the relation

$$a/b = C_{Fx}/C_{Fy} = (D_{11}/D_{22})^{1/4} \tag{13}$$

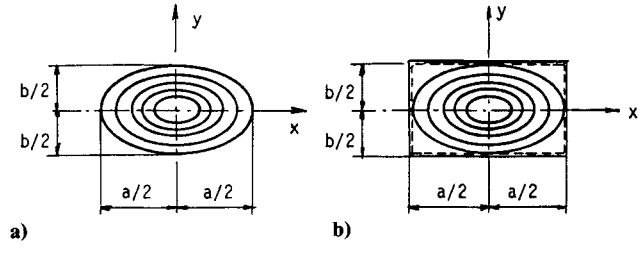

Fig. 2 Shape of the deflected area.

In the Appendix, a similar solution is derived without the assumptions in Eqs. (12) and (13).

In the impact point given by $(x_0,y_0) = (0,0)$, the following applies:

$$W_{jk}(x_0,y_0) = W_{jk}(0,0) = 2/\sqrt{ab} \tag{14}$$

Substitution of Eq. (14) into Eq. (9) gives the plate displacement $w_1(0,0,t)$ at the impacting point:

$$w_1(0,0,t) = \frac{1}{m} \int_0^t F(\tau) \sum_{j=1}^{\infty} \sum_{k=1}^{\infty} \frac{4}{ab\omega_{jk}} \sin[\omega_{jk}(t-\tau)]\, d\tau \tag{15}$$

The double sum in Eq. (15) can be approximated by a continuous integration over j and k in the following way:

$$w_1(0,0,t) = \frac{1}{m} \int_0^t F(\tau) \int_0^{\infty} \int_0^{\infty} \frac{4}{ab\omega_{jk}} \cdot \tfrac{1}{2} \cdot \tfrac{1}{2} \sin[\omega_{jk}(t-\tau)]\, dj\, dk\, d\tau$$

$$= \frac{1}{m} \int_0^t F(\tau) \int_0^{\infty} \int_0^{\infty} \frac{1}{ab\omega_{jk}} \sin[\omega_{jk}(t-\tau)]\, dj\, dk\, d\tau \tag{16}$$

The factors ½ are motivated by Eq. (11). Since ω_{jk} is a continuous smooth function summing over odd cardinal numbers, it can be approximated by one-half of the continuous integral over the same interval. For a specially orthotropic plate, the frequencies ω_{jk} are given[37] by

$$\omega_{jk} = \pi^2 \sqrt{\frac{D_{11}}{m}\left(\frac{j}{a}\right)^4 + \frac{2}{m}(D_{12}+2D_{66})\left(\frac{j}{a}\right)^2\left(\frac{k}{b}\right)^2 + \frac{D_{22}}{m}\left(\frac{k}{b}\right)^4} \tag{17}$$

with Eq. (10) $\Rightarrow a^2/b^2 = \sqrt{D_{11}/D_{22}}$ and

$$A = (D_{12} + 2D_{66})/\sqrt{D_{11}D_{22}} \tag{18}$$

we get

$$ab\omega_{jk} = \frac{\pi^2}{\sqrt{m}} (D_{11}D_{22})^{1/4} \sqrt{j^4 + 2Aj^2k^2 + k^4} \tag{19}$$

If $j \equiv k$ as given by Eq. (12), we obtain

$$ab\omega_{jk} = 2\pi^2 \sqrt{D^*/m}\, jk \tag{20}$$

where the effective plate stiffness D^* is defined by $D^* = [(A + 1)/2] \sqrt{D_{11}D_{22}}$. Note that $A = 1$ for an isotropic plate.

By inserting Eq. (20) into Eq. (16), we obtain

$$w_1(0,0,t) = \frac{1}{m} \int_0^t F(\tau) \int_0^{\infty} \int_0^{\infty} \frac{\sin[\beta(t-\tau)jk]}{2\pi^2\sqrt{D^*/m}\, jk}\, dj\, dk\, d\tau \tag{21}$$

where $\beta = 2\pi^2\sqrt{D^*/m}/(ab)$.

Since $\int_0^{\infty} (\sin ps/s)\, ds = \pi/2$ for $p > 0$,[38] we obtain

$$w_1(0,0,t) = \frac{1}{8\sqrt{mD^*}} \int_0^t F(\tau)\, d\tau \tag{22}$$

where the effective plate stiffness D^* is given in Eq. (20).

Equation (22) can be compared with the solution of Eq. (A8) in the Appendix, which was derived without the assumptions that $j \equiv k$ and $a/b = (D_{11}/D_{22})^{1/4}$.

If we neglect vibrations in the impactor, we may[3] express the displacement of the impactor as

$$w_2(t) = V_0 t - \frac{1}{M} \int_0^t \int_0^{\tau} F(\hat{\tau})\, d\hat{\tau}\, d\tau \text{ with } w_2(0) = 0, \quad \dot{w}_2(0) = V_0 \tag{23}$$

The neglect of vibrations in the impactor requires that the time of load application is much longer than the transition time for internal stress waves in the impactor. This is usually true for balls and short bar metal impactors but not necessarily for longer impactors.

Using Hertz' law of contact, Eq. (1), we obtain the following integral equation:

$$\delta + w_1 - w_2 = 0 \tag{24}$$

where w_1 and w_2 are given by Eqs. (22) and (23).

IV. Solution of the Governing Equations

We can now proceed in the spirit of Zener. Differentiating Eq. (24) twice with respect to time gives

$$\ddot{\delta} + \ddot{w}_1 - \ddot{w}_2 = 0 \tag{25}$$

Inserting Eqs. (22) and (23) and then inserting Eq. (2) gives

$$\left.\begin{aligned} &\frac{d^2\delta}{dt^2} + \frac{1}{8\sqrt{mD^*}} \cdot \frac{3}{2} k_c \delta^{1/2} \frac{d\delta}{dt} + \frac{k_c}{M} \delta^{3/2} = 0 \\ &\text{with initial conditions } \delta(0) = 0, \quad \dot{\delta}(0) = V_0 \end{aligned}\right\} \tag{26}$$

We now introduce the nondimensional variables proposed by Zener:

$$\bar{\delta} = \frac{\delta}{TV_0}, \qquad \bar{t} = t/T \tag{27}$$

where V_0 is the initial velocity of the impactor and T is an unknown time constant. The nondimensional form of Eq. (26) is

$$\left.\begin{aligned} &\frac{d^2\bar{\delta}}{d\bar{t}^2} + \lambda \cdot \frac{3}{2} \bar{\delta}^{1/2} \frac{d\bar{\delta}}{d\bar{t}} + \bar{\delta}^{3/2} = 0 \\ &\bar{\delta}(0) = 0, \quad \frac{d\bar{\delta}(0)}{d\bar{t}} = 1 \end{aligned}\right\} \tag{28}$$

Inserting variables in Eq. (27) into Eq. (28) and identifying coefficients in Eq. (26) gives

$$T = [M/(k_c\sqrt{V_0})]^{2/5} \tag{29}$$

$$\lambda = k_c^{2/5} V_0^{1/5} M^{3/5} / (8\sqrt{mD^*}) \tag{30a}$$

$$\lambda = \left(\frac{4}{3} E_c\right)^{2/5} R^{1/5} V_0^{1/5} M^{3/5} / (8\sqrt{mD^*}) \tag{30b}$$

All of the parameters describing the impact are now included in one single nondimensional parameter λ. The $\bar{\delta}(\bar{t})$ equation, Eq. (28), can be solved numerically for different values of λ. In Fig. 3, dimensionless contact force histories $\bar{\delta}(\bar{t})^{1.5}$ have been plotted for different values of λ.

Inserting Eqs. (27) and (29) into Eqs. (2) and (6) gives

$$F = \left[\left(\frac{4}{3}\right)^{2/5} (E_c)^{2/5} R^{1/5} (MV_0^2)^{3/5}\right] \bar{\delta}^{3/2} \tag{31}$$

$$p_0 = p(0) = \left[\frac{24^{1/5}}{\pi} R^{-3/5} (E_c)^{4/5} (MV_0^2)^{1/5}\right] \bar{\delta}^{1/2} \tag{32}$$

$$I = \int_0^t F(\tau)\, d\tau = MV_0 \cdot \int_0^{\bar{t}} \bar{\delta}^{3/2}(\bar{\tau})\, d\bar{\tau} \tag{33}$$

At the end of impact,

$$I \approx MV_0 \text{ for } \lambda > 1 \tag{34}$$

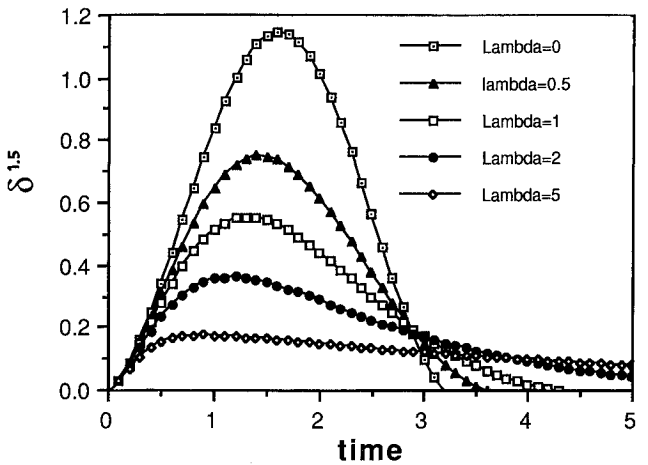

Fig. 3 Dimensionless contact force histories for various lambda values.

By inserting Eq. (33) into Eq. (22), we obtain

$$w_1(0,0,t) = \frac{MV_0}{8\sqrt{mD^*}} \int_0^{\bar{t}} \bar{\delta}^{3/2}\, d\bar{\tau} \tag{35}$$

The solution $\bar{\delta}(\bar{t})$ contains all of the information necessary to compute contact force, contact pressure, displacement, shear load, and bending stresses in the impact point.

For this purpose a short FORTRAN program "impact" has been written. Equation (28) can be written as a system of two ordinary differential equations. The program "impact" is based on an existing standard program for the solution of such systems. The standard program has been adopted to give all functions of $\bar{\delta}$ that are required.

V. Flexural Wave Propagation

As observed by Takeda,[39] a very low amplitude tensile stress wave propagates from the impact point during the first microseconds. We are, however, mainly interested in the flexural deformation of the plate that results in much higher stresses.

The velocity in thin plates for plane flexural waves in the direction θ and with a wavelength much longer than the plate thickness is given[40] by

$$C_F(\theta) = \left(\frac{D(\theta)}{m}\right)^{1/4} \sqrt{\omega} \tag{36}$$

However, the shear wave velocity $C_s(\theta)$ puts an upper limit to the in-plane propagation of transversal disturbances:

$$C_S(\theta) = \sqrt{G_{rz}(\theta)/\rho_1} \tag{37}$$

For homogenous isotropic and orthotropic materials, a more correct velocity limit is the Rayleigh wave speed C_R that in homogeneous isotropic media is slightly lower than C_S.[41] Experimental results by Takeda[39] show that the leading edge of flexural disturbances in cross-ply glass/epoxy laminates also propagates at a velocity slightly lower than C_S (estimated from material data).

To compute the velocity of flexural waves, we note that for a certain j, k

$$a/2 = \int_0^t C_{Fjk}\, d\tau = \int_0^t \left(\frac{D_{11}}{m}\right)^{1/4} \sqrt{\omega_{jk}}\, d\tau \tag{38}$$

From Eq. (20), we have

$$\omega_{jk} = \frac{\pi^2}{\sqrt{m}} \frac{(D_{11}D_{22})^{1/4}\sqrt{2(A+1)}}{ab} jk$$

$$= \frac{\pi^2}{a^2} \sqrt{\frac{D_{11}}{m}} \sqrt{2(A+1)}\, jk \tag{39}$$

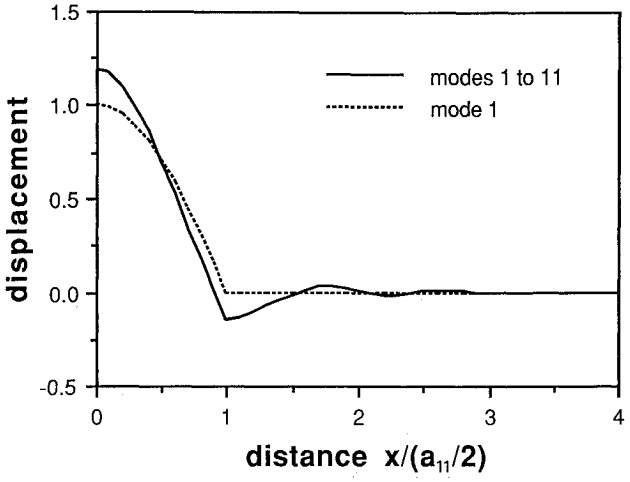

Fig. 4 Normalized predicted displacement vs distance from the impact center.

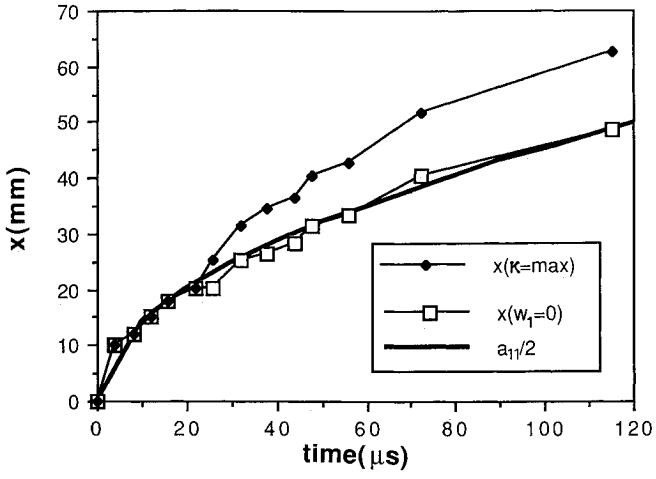

Fig. 5 Propagation of flexural waves in an impacted glass/epoxy plate. Comparison with experimentally determined position of κ_{max} and first node line ($w_1 = 0$) with the front of the first wave mode ($a_{11}/2$).

since $a/b = (D_{11}/D_{22})^{1/4}$ according to Eq. (13).

Inserting Eq. (39) into Eq. (38) implies

$$\frac{da}{d\tau} = 2C_{Fxjk} = 2\frac{\pi}{a}\sqrt{\frac{D_{11}}{m}}\,[2(A+1)]^{1/4}\sqrt{jk} \tag{40}$$

$$a_{jk} = 2\sqrt{\pi}\left(\frac{D_{11}}{m}\right)^{1/4}[2(A+1)]^{1/8}(jk)^{1/4}\sqrt{t} \tag{41}$$

Inserting this result into Eq. (40) gives

$$C_{Fxjk} = \frac{\sqrt{\pi}}{2}\left(\frac{D_{11}}{m}\right)^{1/4}[2(A+1)]^{1/8}(jk)^{1/4}/\sqrt{t} \tag{42}$$

Equation (41) describes how far from the impact center a certain mode front has reached. Inserted in Eq. (10), it can be used to determine the shape of an individual mode. Figure 4 shows the theoretical displacement form when one and six modes are included in the summation. Amplitudes and distance from impact center are normalized with respect to the first mode. The displacements are not significantly changed by adding higher modes. Figure 4 is almost identical to displacement forms observed experimentally by Fällström et al.[36,42] Reference 42 also included analytical solutions for an isotropic plate impacted by a unit pulse or a sine wave pulse. These solutions, which essentially are zeroth order Bessel functions, agree with Fig. 4, except that they are smoother. Furthermore, after completed impact, the central displacement is identical to Eq. (35). It is noted from Fig. 4 that large flexural strains occur in the impact center and in a flexural wave slightly ahead of the first node line that can be approximated with the position of the first mode wave front.

To examine the validity of Eq. (41), a comparison was made with experimental results by Takeda,[39] Fällström et al.,[42] and Fällström.[43] Takeda used strain gauges to measure the position of the main flexural stress wave (κ_{max}), whereas Fällström et al. provided photographs showing the whole displacement field, making it possible to determine the positions of the first node line and maximum curvature. These results were compared with the predicted position of the wave front of mode 1 ($a_{11}/2$ and $b_{11}/2$), and an excellent agreement was found. The comparison with Fällström et al. is given in Fig. 5. Finally, we note that Eq. (41) can be used to determine when influence from plate boundaries is to be expected.

VI. Plate Stresses and Strains

Differentiating the eigenfunctions of Eq. (10) twice and then proceeding in the same way as when deriving displacement results in infinite central curvature. A previous approximation[30] proposed by the author has shown a bad correlation to experimental data.[1] Instead, an expression is sought by generalizing a solution by Sneddon[26] for isotropic nonshear-deformable plates. This solution was applied and experimentally verified by Schweiger[27] for Hertzian impacts on isotropic plates. First, we note that Eq. (22) is equal to the classical solution by Sneddon,[26] Zener,[25] and originally by Boussinesq,[44] if the isotropic plate stiffness D is replaced by the effective plate stiffness D^*. Second, we note that Sneddon's cylindrically symmetrical solution $w_1(\tilde{r},t)$ given in the coordinates $\tilde{x}$, $\tilde{y}$

$$\tilde{x} = \tilde{r}\cos\theta, \qquad \tilde{y} = \tilde{r}\sin\theta \tag{43}$$

can be transformed to an elliptical system x, y by projecting the coordinates according to the relation of the corresponding flexural wave velocities:

$$x = (D_{11}/D^*)^{1/4}\tilde{x}, \quad y = (D_{22}/D^*)^{1/4}\tilde{y} \tag{44}$$

In fact, such a solution seems more suited for describing the displacement field of an orthotropic plate than the rectangular plate approximation. Further support for this intuitive conclusion can be found by comparing with the displacement fields observed experimentally by Fällström et al.[36]

To derive the time histories of central displacement and central curvature of an isotropic plate, Sheddon used Hankel transformations. Using serial expansions of improper integrals, Sneddon derived the following approximate expression for the central curvature during the impact:

$$\kappa_{\tilde{x}}(0,0,t) = \kappa_{\tilde{y}}(0,0,t) = \kappa_{\tilde{r}}(0,\theta,t)$$
$$= \frac{\partial^2 w_1(0,\theta,t)}{\partial \tilde{r}^2} = -\frac{\dot{w}_1(0,0,t)}{\pi}\sqrt{\frac{m}{D}}\,[\ln(t_0/t) - 0.4228] \tag{45}$$

for $t \le t_c$ (t_c = contact time) provided that $t_0/t \ll 1$ where

$$t_0 = c^2\sqrt{m/D}/4 \tag{46}$$

After completed impact, the solution is

$$\kappa_{\tilde{r}}(0,0,t) = -\frac{\dot{w}_1(0,0,t)}{\pi}\sqrt{\frac{m}{D}}\,[\ln(1 - t_c/t)] \tag{47}$$

However, $\dot{w}_1(0,0,t) = 0$ when $t > t_c$ if no boundary reflections have occurred.

We note that the condition $t_0/t \ll 1$ is equivalent to the condition that the area affected by contact stresses is negligible in comparison with the area inside the first node line, which

for the orthotropic case can be approximated using Eq. (41). The resulting condition is

$$\frac{\pi c^2}{a_{11}b_{11}} = \frac{c^2\sqrt{m}}{4(D_{11}D_{22})^{1/4}[2(A+1)]^{1/4}t} \ll 1 \tag{48}$$

Differentiating Eq. (45) with respect to x considering Eq. (44), replacing D by D^* in Eq. (20), and using Eqs. (7) and (27) results in the following expression for the central curvature:

$$\kappa_x(0,0,t) = \frac{\partial^2 w_1(0,0,t)}{\partial x^2} = \frac{F}{8\pi\sqrt{D_{11}D^*}}\left[\ln\left(\frac{RV_0}{4}\frac{\bar{\delta}}{\bar{t}}\sqrt{\frac{m}{D^*}}\right) - 0.4228\right] \tag{49}$$

for $t \le t_c$ where F is given by Eq. (31) and D^* by Eq. (20). The κ_y is obtained by replacing D_{11} with D_{22}. Using classical laminated plate theory, the flexural strains in midplane symmetric plates are obtained from

$$\epsilon_x(0,0,z,t) = z\kappa_x(0,0,t), \quad \epsilon_y(0,0,z,t) = z\kappa_y(0,0,t) \tag{50}$$

VII. Some Observations on the Model

Several observations can be made from the numerical solutions of Eq. (28).

By studying the impulse I, Eq. (33), transferred to the plate we note that after completed impact $I = 2MV_0$ for $\lambda = 0$ and $I \approx MV_0$ for $\lambda > 1$. Due to the conservation of momentum, the resulting impactor rebound velocity $\dot{W}_2$ is $\dot{W}_2 = -V_0$ for $\lambda = 0$ and $\dot{W}_2 \approx 0$ for $\lambda > 1$. Thus, for $\lambda > 1$ the behavior is similar to that after an inelastic impact. This motivated Zener to designate λ as the "inelasticity parameter." Since the plate displacement w_1 is proportional to the impulse, it will be proportional to impactor mass and velocity if $\lambda > 1$.

The conclusion that the impact is essentially inelastic for $\lambda > 1$ is supported by observations by Petersen,[13] who used finite element analysis to study an impact problem with $\lambda \approx 1.5$. He found that changing the contact law from Hertzian to inelastic had virtually no influence on the plate response.

It can be seen from Eqs. (33) and (35) that, if the kinetic energy $MV_0^2/2$ of the impactor is kept constant while the impact velocity is increased, zero displacement is, as expected, approached since the transferred impulse I limited by $I \le 2MV_0 = 2MV_0^2/V_0$ decreases. In this case, we approach pure perforation problems.

The model can be used for parametric studies. Varying parametric ratios in the interval 0.1–10 gives the following approximate formulas for a spherical impactor:

$$\bar{F}_{\max} \approx \overline{(\rho_2/\rho_1)}^{-0.25}\,\overline{(MV_0^2)}^{0.53}(\bar{R})^{-0.52}(\bar{E}_c)^{0.10}(\bar{h})^{0.70}(\bar{E}_F)^{0.34} \tag{51}$$

where $\bar{E}_F = 12\sqrt{D_{11}D_{22}}/h^3$.

All parameters are normalized with respect to some original value where λ is equal to unity. The influence of stiffnesses (especially contact stiffness) on $\bar{F}_{\max}$ is very small.

Although the governing differential equation cannot be solved analytically, some exact results can be found for $\lambda = 0$, and some limits can be established for other cases.

$\lambda = 0$: Multiplying Eq. (28) by $2\bar{\delta}' = 2d\bar{\delta}/d\bar{t}$ and then integrating and considering initial conditions gives

Maximum $\bar{\delta}$:

$$\bar{\delta}_m = \left(\frac{5}{4}\right)^{2/5} \tag{52}$$

Final velocity $\bar{\delta}'$:

$$\bar{\delta}' = \underset{(+)}{-}1 \tag{53}$$

$\lambda > 0$: Integrating Eq. (28) and considering initial conditions gives

$$\bar{\delta}^{3/2} = \frac{1}{\lambda}[1 - \bar{\delta}' - I(\bar{t})] \tag{54}$$

Maximum $\bar{\delta}^{3/2}$:

$$\bar{\delta}' = 0 \Rightarrow \bar{\delta}_m^{3/2} = \frac{1}{\lambda}[1 - I(\bar{t})] < \frac{1}{\lambda} \tag{55}$$

Final velocity:

$$\bar{\delta} = 0 \Rightarrow \bar{\delta}' = 1 - I(\bar{t}) \tag{56}$$

For physical reasons and from numerical observations we know that $1 < I(\bar{t}) < 2$. Thus

$$-1 < \bar{\delta}' < 0 \tag{57}$$

The following approximation for Eq. (55) was found to be successful for $\lambda > 1$:

$$\bar{\delta}_m^{*3/2} \approx (1 - 0.4442/\lambda^q)/\lambda \tag{58}$$

Setting $q = 0.8$ results in an error of less than 3% for $1 < \lambda < 15$.

VIII. Comparison with Other Studies

To verify the model, an initial experimental study[1] was initiated since no studies could be found where contact force, displacement, and strains under the impact force were recorded simultanously under wave-controlled conditions. In these experiments an orthotropic carbon/epoxy laminated plate was impacted with a 30 g pendulum-mounted steel ball at five different impact velocities ranging from 0.38 to 1.89 m/s. The plate displacement was measured by studying a series of short pulse laser holograms from a number of repeated identical impacts. Flexural strains were recorded using a cross-mounted strain gauge and "contact force" using an accelerometer on the impactor. The plate size was chosen to guarantee negligible boundary influence during the major part of the impact times.

Using ply data and experimental data in Ref. 1 results in the following data for the impacted plate:

$D_{11} = 632.2$ Nm
$D_{12} = 198.0$ Nm
$D_{16} = D_{26} \approx 0$
$D_{22} = 273.5$ Nm
$D_{66} = 214.6$ Nm
$m = 7.36$ kg/m^2
Dimensions: $400 \times 500 \times 4.572$ mm

The data of the impacting steel ball were $M = 30$ g and $R = 9.5$ mm.

In the experiments, λ ranged from 0.90 to 1.25 and the time constant T from 49 to 68 μs. Contact force and displacements were predicted with high accuracy except for a small time difference (see Fig. 6). Using the theory in Ref. 30, flexural strains were only predicted qualitatively. However, when using Eq. (50), the flexural strains are predicted with an error of a few percent (see Fig. 7). A linear relation was observed between flexural strains and the impact velocity. A similar linear dependency has been predicted and experimentally verified by Qian et al.[45] who considered scaling laws on plate impact problems.

Doyle[46] experimentally determined the time-force history with the help of fast Fourier transform (FFT) analysis of signals from a number of strain gauges. A 12.7-mm steel ball with a velocity of 2.3 m/s was used to impact a seven layer [0/90] 3M Scotch ply glass epoxy laminate of dimensions $406 \times 406 \times 1.78$ mm. The contact-force history was predicted

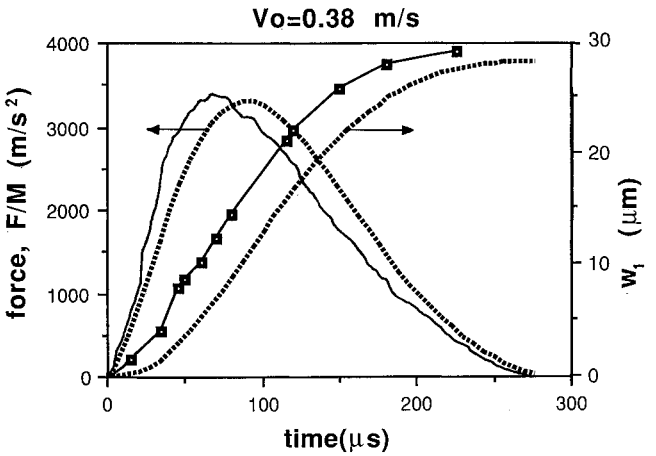

Fig. 6 Predicted (dotted) and measured contact force and center displacement in a $(45/0/-45)_{6S}$ laminate.

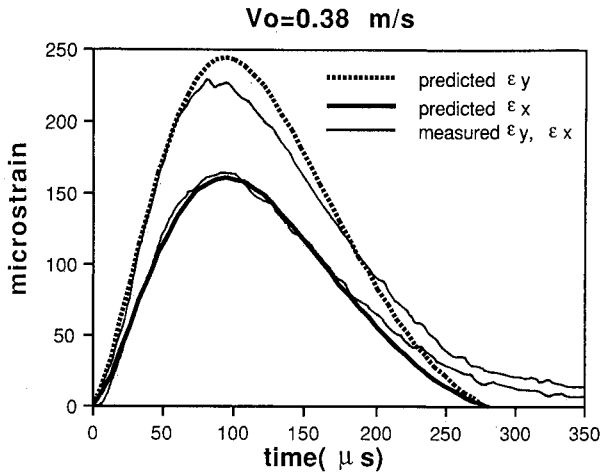

Fig. 7 Predicted (dotted) and measured flexural strains in a $(45/0/-45)_{6S}$ laminate.

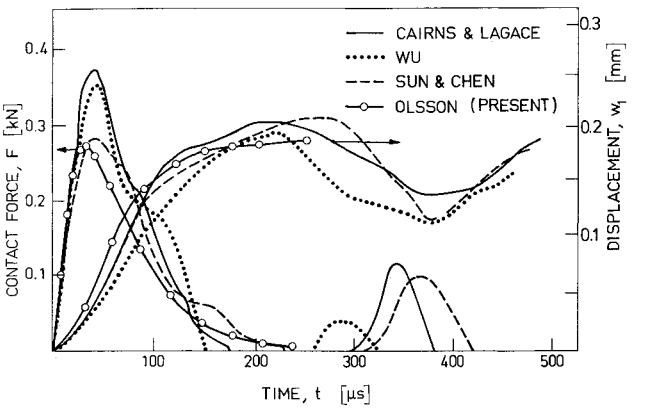

Fig. 8 Contact force and center displacement in a (0/90/0/90/0) laminate predicted from the present theory and a number of numerical analyses.[20,17,47]

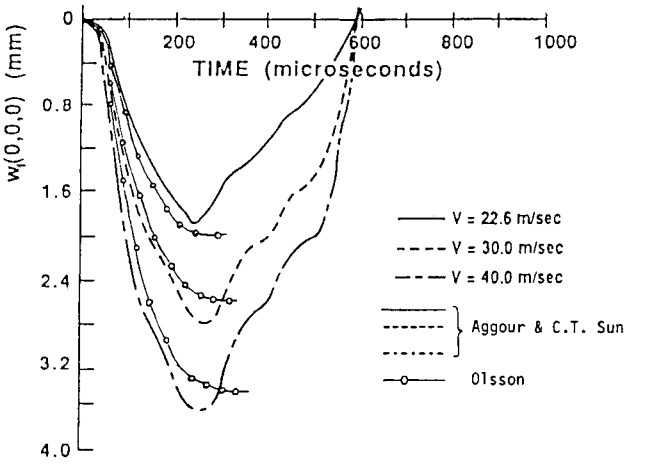

Fig. 9 Center displacement for various impact velocities predicted by the present theory and by finite element analysis by Aggour and Sun.[14]

accurately with the present model, except for a small time lag, with a difference in predicted and measured contact force of 8%. The full comparison is given in Ref. 30.

The model has also been compared with a number of numerical solutions. Cairns and Lagace[20] used a quick Rayleigh-Ritz energy method to solve the finite-varying initial problem for anisotropic Mindlin plates. They assumed a Hertzian contact law. Several impact cases were studied with a number of different impactors, plates, and boundary conditions. One of the cases that also has been studied by Sun and Chen[17] and Wu[47] was the impact on a 200 × 200 mm $[0/90/0/90/0]_s$ graphite/epoxy (T300/934) plate.

The ply data given in Ref. 20 result in the following plate properties:

$D_{11} = 154.9$ Nm
$D_{12} = 4.760$ Nm
$m = 4.132$ kg/m^2
$D_{22} = 91.4$ Nm
$D_{66} = 8.970$ Nm
$h = 2.69$ mm

The impactor was a steel ball with the following data: $R = 6.35$ mm, $V_0 = 3.0$ m/s, and $M = 8.30$ g. Using Eqs. (5) and (8b) gives $E_c = 9.72$ GPa. Impact parameters were $\lambda = 2.08$ and $T = 29.3$ μs.

The comparisons of contact force and central plate displacement predicted from the present model are given in Fig. 8. Further comparisons are given in Ref. 30.

Aggour and Sun[14] used a two-dimensional finite element analysis to study displacement, normal stress, and average shear stress in two composite plates impacted elastically by a steel cylinder at various velocities. The program included shear deformation. The response of [0/90/0] glass-epoxy plates was studied at three different impact velocities.

Using the ply data for 1.27 mm plies given in Ref. 14 results in the following plate properties:

$D_{11} = 181.3$ Nm
$D_{12} = 9.65$ Nm
$m = 7.245$ kg/m^2
$D_{22} = 44.1$ Nm
$D_{66} = 19.03$ Nm
$h = 3.81$ mm
Dimensions: 140 mm × 140 mm clamped-clamped

The impactor was a 9.525-mm-diam blunt-ended steel cylinder with a Hertzian contact behavior. The load was uniformly distributed over the cylinder end area; $M = 14.17$ g, contact stiffness plate impactor $k_c = 100 \cdot 10^6$ N/m$^{1.5}$.

The comparisons with the present solution are given in Fig. 9; impact parameters: $\lambda = 1.29$–1.45, $T = 55$–62 μs.

Sun and Liou[16] used a three-dimensional finite element method to analyze stresses and displacements in cross-ply 140 × 140 mm laminates with three, four, and five plies. One of the cases studied was a (0/90/0) graphite/epoxy laminate where the ply data given in Ref. 16 results in the following

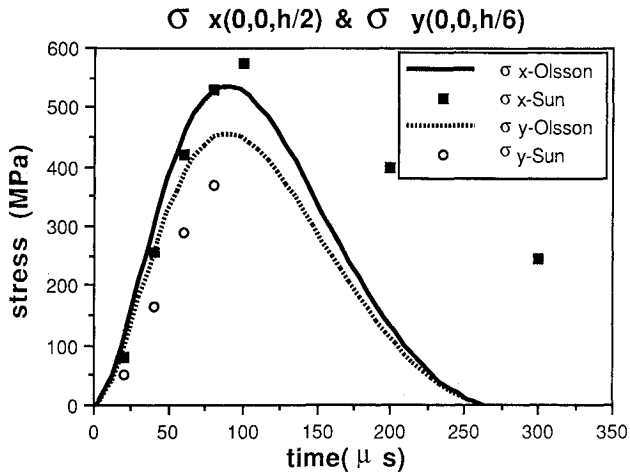

Fig. 10 Flexural stresses in a (0/90/0) laminate predicted by the present theory and a three-dimensional finite element method by Sun and Liou.[16]

laminate data:

$D_{11} = 641$ Nm
$D_{12} = 19.2$ Nm
$m = 6.134$ kg/m^2
$D_{22} = 86.3$ Nm
$D_{66} = 21.4$ Nm
$h = 3.81$ mm

The impactor and contact load had the same data as given in the preceding example: impact velocity, $V_0 = 22.6$ m/s; impact parameters, $\lambda = 0.952$, $T = 61.63$ μs.

Since the contact radius c is constant in this example, Eq. (49) cannot be used in its original form [compare Eqs. (45) and (46)]. In the Hertzian theory $RV_0\bar{\delta}/\bar{t}$ is equal to c^2/t according to Eqs. (7) and (27). In the present case, $RV_0\bar{\delta}/\bar{t}$ is replaced by c^2/t where c is the impactor cylinder radius 9.525 mm/2.

Comparison of central stresses predicted by the present model is given in Fig. 10. The fact that the predicted magnitudes of σ_x and σ_y coincide is merely a coinsidence resulting from z coordinates chosen for computing the stresses. It should be noted that the stresses predicted from the present theory and by the three-dimensional finite element model are not fully comparable since the present model does not consider three-dimensional effects and assumes a contact area that is small compared with the plate thickness.

Sun and Liou also studied the central displacement of the plate described earlier when the thickness was scaled to $h = 3.81$, 5.72, and 7.62 mm. The computed maximum values were 2.4, 1.3, and 0.80 mm. The values predicted from the present model are 2.7, 1.3, and 0.76 mm.

The influence of neglecting shear deformations can be studies by comparing with Mittal's[29] shear deformable theory for transversally isotropic plates. In this theory, T_0 and λ are completely interchangeable with T and λ in the present theory. In addition, Mittal includes a shear parameter that can be rewritten as

$$\beta' = \frac{h\sqrt{3E_f\rho_1}}{5TG_t} \tag{59}$$

where $E_f = 12D/h^3$. By studying the results given by Mittal, the influence of shear is seen to be small for $\beta < 0.1$. It is noted that $\beta' < 0.1$ for all cases studied in this section. It is believed to be valid for most impacts on thin laminated plates.

IX. Conclusions

The analytical method presented in this article seems to be able to predict the time response at the impact point during the primary impact in a specially orthotropic plate impacted by an impactor with a semispherical tip, under the condition that major flexural waves have not yet been reflected from the boundaries. Predicted displacements, flexural strains, or stresses and contact force (and, indirectly, contact stresses) are in good agreement with presented numerical methods and experimental results.

The character of the impact has been shown to be controlled by the single nondimensional parameter λ that depends on parameters of the plate and the impactor as well as the impact velocity. In general, λ increases with increasing kinetic energy and contact stiffness of the impactor and decreases with increasing density and stiffness of the plate. Increasing λ shortens the loading phase and prolongs the unloading phase of the time-force curve. For $\lambda > 1$, which is the most common for impacted composite plates, the impact is almost inelastic and the maximum displacement is directly proportional to the mass and velocity of the impactor. Final displacement increases if the plate-impactor contact stiffness is reduced to such an extent that λ falls below unity. In the case $\lambda = 0$, displacement is doubled compared with cases where $\lambda > 1$.

An approximate parametric formula shows that transversal Young's modulus has a small influence on the contact force. The contact force is mainly influenced by impact energy, impactor radius, and plate thickness. In apparent contradiction, the contact force increases with reduced impactor radius and reduced impactor density. The latter was also observed in a numerical study by Cairns and Lagace.[20]

A comparison with a number of numerical analyses indicates that boundary conditions usually have a small influence on central displacement, flexural strains, and contact force during the primary impact in short time (i.e., low mass) impacts on reasonably large laminates.

The velocity of the flexural waves is shown to be proportional to the square root of the wave mode number (i.e., the number of half cosine waves) and inversely proportional to square root of time. This is a special result for flexural waves in an area of propagating wave fronts, since in such an area the wavelength for a certain mode number is constantly growing. The formula presented is supported by a number of experimental results.

A comparison with a solution for shear-deformable transversally isotropic plates indicates that shear effects usually are negligible in laminated plates.

According to the present analysis, the common method of relating impact response and damage to impact energy is inadequate since mass and velocity are independent parameters. Such a use can only be justified if repeated experiments yield the same response for different combinations of mass and velocity having the same impact energies.

X. Remarks

After the submission of this article, the predictions of the present model were verified in an experimental study by varying all of the parameters involved in the solution. The study was presented in Ref. 48.

Appendix

It is possible to derive a solution w_1 that is approximately equal to Eq. (22) without making the assumptions $a^2/b^2 = \sqrt{D_{11}/D_{22}}$ and $j \equiv k$:

$$\omega_{jk} = \pi^2 \sqrt{\frac{D_{11}}{m}\left(\frac{j}{a}\right)^4 + \frac{2}{m}(D_{12} + 2D_{66})\left(\frac{j}{a}\right)^2\left(\frac{k}{b}\right)^2 + \frac{D_{22}}{m}\left(\frac{k}{b}\right)^4} \tag{A1}$$

By making the substitution

$$x = \left(\frac{D_{11}}{m}\right)^{1/4}\left(\frac{j}{a}\right) \text{ and } y = \left(\frac{D_{22}}{m}\right)^{1/4}\left(\frac{k}{b}\right) \tag{A2}$$

$$\omega_{xy} = \pi^2\sqrt{x^4 + 2Ax^2y^2 + y^4} \text{ where } A = (D_{12} + 2D_{66})/\sqrt{D_{11}D_{22}} \tag{A3}$$

We may now write

$$\int_0^\infty\int_0^\infty \frac{1}{ab\omega_{jk}}\,dj\,dk = \frac{\sqrt{m}}{(D_{11}D_{22})^{1/4}}\int_0^\infty\int_0^\infty \frac{dx\,dy}{\omega_{xy}}$$

Substituting the preceding expressions in Eq. (16) gives

$$w_1(0,0,t) = \frac{1}{m}\int_0^t F(\tau)\int_0^\infty\int_0^\infty \frac{\sqrt{m}}{(D_{11}D_{22})^{1/4}}\frac{\sin[\omega_{xy}(t-\tau)]}{\omega_{xy}}\,dx\,dy\,d\tau \tag{A4}$$

By introducing cylindrical coordinates $x = r\cos\theta$, $y = r\sin\theta$, and then setting $s = r^2$, $ds = 2r\,dr$, $f(\tau) = t - \tau$, and

$$h(\theta) = 1/\sqrt{\cos^4\theta + 2A\cos^2\theta\sin^2\theta + \sin^4\theta}$$
$$= 1/\sqrt{1 + [(A-1)/2]\sin^2 2\theta} \tag{A5}$$

$$w_1(0,0,t)$$
$$= \frac{1}{\sqrt{m}(D_{11}D_{22})^{1/4}}\int_0^t F(\tau)\int_0^{\pi/2}\int_0^\infty \frac{h(\theta)}{2\pi^2}\sin\left|\frac{f(\tau)}{h(\theta)}s\right|\frac{1}{s}\,ds\,d\theta\,d\tau$$
$$= \frac{1}{8\sqrt{m}(D_{11}D_{22})^{1/4}}\int_0^t F(\tau)\int_0^{\pi/2}\frac{h(\theta)}{\pi/2}\,d\theta\,d\tau$$
$$\left(\text{since}\int_0^\infty \frac{\sin ps}{s}\,ds = \frac{\pi}{2}\right) \tag{A6}$$

By the substitution $\phi = 2\theta$, we obtain the solution from an elliptic integral[49]:

$$\int_0^{\pi/2}\frac{h(\theta)}{\pi/2}\,d\theta$$
$$= \begin{cases} 2K[\sqrt{(1-A)/2}]/\pi & \text{if } 0 \le A < 1 \\ 1 & \text{if } A = 1 \\ 2\sqrt{2/(A+1)}\,K[\sqrt{(A-1)/(A+1)}]/\pi & \text{if } A > 1 \end{cases} \tag{A7}$$

where $K(k)$ is the complete elliptic integral of the first kind.[38]

Acknowledgments

Economic support for the work was provided by the Swedish Defence Materials Administration. The author wishes to acknowledge the assistance with experiments and data from the Division of Experimental Mechanics at Luleå Technical University, especially Per Gren and K.-E. Fällström. Pavel Sindelar encouraged the work and has been a valuable discussion partner.

References

[1]Olsson, R., "Pilot Study of the Dynamic Impact Response of a Composite Plate," Aeronautical Research Inst. of Sweden, FFA TN 1990-27, Stockholm, Oct. 1990.

[2]Cantwell, W. J., and Morton, I., "Comparison of the Low and High Velocity Impact Responce of CFRP," *Composites,* Vol. 20, No. 6, 1989, pp. 545–551.

[3]Goldsmith, W., *Impact,* Edward Arnold, London, 1960, Chap. IV, pp. 82–144.

[4]Shivakumar, K. N., Elber, W., and Illg, W., "Prediction of Impact Force and Duration Due to Low-Velocity Impact on Circular Composite Laminates," *Journal of Applied Mechanics,* Vol. 52, No. 3, 1985, pp. 674–680.

[5]Kelkar, A., Elber, W., and Raju, I. S., "Large Deflection Behaviour of Quasi-Isotropic Laminates under Low-Velocity Impact Type Point Loading," *Proceedings of the AIAA/ASME/ASCE/AHS 26th Structures, Structural Dynamics, and Materials Conference,* Pt. 1, AIAA, New York, 1985, pp. 432–441; also AIAA Paper 85-0723.

[6]Bucinell, R. B., Nuismer, R., and Koury, J. L., "Response of Composite Plates to Quasi-Static Impact Events," *Composite Materials: Fatigue and Fracture (Third Volume), ASTM STP 1110,* edited by T. K. O'Brien, American Society for Testing and Material, Philadelphia, PA, 1991, pp. 528–549.

[7]Wang, C-Y., "A Study of Impact Damage in Composite Laminates," Ph.D. Thesis, Univ. of Texas, Austin, TX, May 1989.

[8]Daniel, I. M., and Wooh, S. C., "Deformation and Damage of Composite Plates Under Impact Loading," *Proceedings of the International Symposium on Composite Materials and Structures,* edited by T. T. Loo and C. T. Sun, Technomic, Lancaster, PA, 1986, pp. 630–637.

[9]Sjöblom, P. O., Hartness, I. T., and Cordell, T. M., "On Low-Velocity Impact Testing of Composite Materials," *Journal of Composite Materials,* Vol. 22, No. 1, 1988, pp. 30–52.

[10]Reed, P. E., and Turner, S., "Flexed Plate Impact, Pt. 7: Low Energy and Excess Energy Impacts on Carbon Fibre-Reinforced Polymer Composites," *Composites,* Vol. 19, No. 3, 1988, pp. 193–203.

[11]Karas, K., "Platten Under Seitlichem Stoss," *Ingenieur-Archiv,* Vol. 10, No. 4, 1939, pp. 237–250.

[12]Wu, H.-Y. T., and Springer, G. S., "Impact Induced Stresses, Strains and Delaminations in Composite Plates," *Journal of Composite Materials,* Vol. 22, No. 6, 1988, pp. 533–560.

[13]Petersen, B. R., "Finite Element Analysis of Composite Plate Impacted by a Projectile," Ph.D. Dissertation, Univ. of Florida, Gainesville, FL, 1985.

[14]Aggour, H., and Sun, C. T., "Finite Element Analysis of a Laminated Composite Plate Subjected to Circularly Distributed Central Impact Loading," *Computers and Structures,* Vol. 28, No. 6, 1988, pp. 729–736.

[15]Wu, H.-Y. T., and Chang, F.-K., "Transient Dynamic Analysis of a Laminated Composite Plates Subjected to Transverse Impact," *Composites and Structures,* Vol. 31, No. 3, 1989, pp. 453–466.

[16]Sun, C. T., and Liou, W. J., "Investigation of Laminated Composite Plates Under Impact Dynamic Loading Using a Three-Dimensional Hybrid Stress Finite Element Method," *Composite and Structures,* Vol. 33, No. 3, 1989, pp. 879–884.

[17]Sun, C. T., and Chen, J. K., "On the Impact of Initially Stressed Composite Laminates," *Journal of Composite Materials,* Vol. 19, No. 6, 1985, pp. 490–509.

[18]Chen, P. C., and Ramkumar, R. L., "Static and Dynamic Analysis of Clamped Orthotropic Plates Using Lagrangian Multiplier Technique," *AIAA Journal,* Vol. 25, No. 2, 1987, pp. 316–323.

[19]Dobyns, A. L., "Analysis of Simply-Supported Orthotropic Plates Subject to Static and Dynamic Loads," *AIAA Journal,* Vol. 19, No. 5, 1981, pp. 642–650.

[20]Cairns, D. S., and Lagace, P. A., "Transient Response of Graphite/Epoxy and Kevlar/Epoxy Laminates Subjected to Impact," *AIAA Journal,* Vol. 27, No. 11, 1989, pp. 1590–1596.

[21]Sun, C. T., and Chattopadhyay, S., "Dynamic Response of Anisotropic Laminated Plates Under Initial Stress to Impact of a Mass," *Journal of Applied Mechanics,* Vol. 43, No. 3, 1975, pp. 693–698.

[22]Qian, Y., and Swanson, S. R., "A Comparison of Solution Techniques for Impact Response of Composite Plates," *Composite Structures,* Vol. 14, No. 3, 1990, pp. 177–192.

[23]Christoforou, A. P., and Swanson, S. R., "Analysis of Simply-Supported Orthotropic Cylindrical Shells Subject to Lateral Impact Loads," *Journal of Applied Mechanics,* Vol. 57, No. 2, 1990, pp. 376–382.

[24]Lin, H. J., and Lee, Y. J., "On the Inelastic Impact of Composite Laminated Plate and Shell Structures," *Composite Structures,* Vol. 14, 1990, No. 2, pp. 89–111.

[25]Zener, C., "The Intrinsic Inelasticity of Large Plates," *Physical Review,* Vol. 59, April 1941, pp. 669–673.

[26]Sneddon, I. N., "The Symmetrical Vibrations of a Thin Elastic Plate," *Proceedings of the Cambridge Philosophical Society,* Vol. 41, No. 1, 1945, pp. 27–43.

[27]Schweiger, H., "Maximale Beansprochung schlagartig belasteter elastischer Platten," Deutsche Versuchsanstalt Für Luft- und Raumfahrt, FB 66-33, Mülheim, May 1966.

[28]Schweiger, H., "Vereinfachte Theorie des Elastischen Biegestosses auf eine Dünne Platte und ihre Experimentelle Überprüfung," *Forschung im Ingenieurswesen,* Vol. 41, No. 4, 1975, pp. 122–132.

[29]Mittal, R. K., "A Simplified Analysis of the Effect of Transverse Shear on the Response of Elastic Plates to Impact Loading," *Journal of Solids and Structures,* Vol. 23, No. 8, 1987, pp. 1191–1203.

[30]Olsson, R., "Impact Response of Orthotropic Composite Plates Predicted by a One-Parameter Differential Equation," Aeronautical Research Inst. of Sweden, FFA TN 1989-07, Stockholm, 1989.

[31]Rechak, S., "Effect of Adhesive Layers on Impact Damage and

Dynamic Response in Composite Laminates," Ph.D. Dissertation, Purdue Univ., West Lafayette, IN, 1986,

[32]Greszczuk, L. B., *Impact Dynamics,* Wiley, New York, 1982, Chap. 3, pp. 55-94.

[33]Tan, T. M., and Sun, C. T., "Use of Statical Indentation Laws in the Impact Analysis of Laminated Composite Plates," *Journal of Applied Mechanics,* Vol. 52, No. 1, 1985, pp. 6-12.

[34]Henriksson, A., "Transverse Compressive Behaviour of Carbon-Epoxy Laminates and Its Influence on Contact Laws," The Aeronautical Research Institute of Sweden, FFA TN 1990-26, Stockholm, Oct. 1990.

[35]Soedel, W., *Vibrations of Shells and Plates,* Marcel Dekker, New York, 1981, pp. 229-233.

[36]Fällström, K.-E., Lindgren, L.-E., Molin, N.-E., and Wåhlin, A., "Transient Bending Waves in Anisotropic Plates Studied by Hologram Interferometry," *Journal of Experimental Mechanics,* Vol. 29, No. 4, 1989, pp. 409-413.

[37]Jones, R. M., *Mechanics of Composite Materials,* Hemisphere, Washington, DC, 1975.

[38]Spiegel, M. R., *Mathematical Handbook,* Schaum/McGraw-Hill, New York, 1968.

[39]Takeda, N., "Experimental Studies of the Delamination Mechanisms in Impacted Fiber-Reinforced Composite Plates," Ph.D. Thesis, Univ. of Florida, Gainesville, FL, 1980.

[40]Skudrzuk, E., *Simple and Complex Vibratory Systems,* Pennsylvania State Univ. Press, University Park, PA, 1968.

[41]Chow, T. S., "On the Propagation of Flexural Waves in an Orthotropic Laminated Plate and Its Response to an Impulsive Load," *Journal of Composite Materials,* Vol. 5, July 1971, pp. 306-319.

[42]Fällström, K.-E., Gustavsson, H., Molin, N.-E., and Wåhlin, A., "Transient Bending Waves in Plates Studied by Hologram Interferometry," *Journal of Experimental Mechanics,* Vol. 29, No. 4, 1989, pp. 378-387.

[43]Fällström, K.-E., private communication, 1988.

[44]Boussinesq, J. N., *Application des Potentiels à l'Étude de l'Équilibre et du Mouvement des Solides Élastiques,* Gauthier-Villars, Paris, 1885, pp. 464-480.

[45]Qian, Y., Swanson, S. R., Nuismer, R. J., and Bucinell, R. B., "An Experimental Study of Scaling Rules for Impact Damage in Fiber Composites," *Journal of Composite Materials,* Vol. 24, No. 5, 1990, pp. 559-570.

[46]Doyle, J. F., "Experimentally Determining the Contact Force During the Transverse Impact of an Orthotropic Plate," *Journal of Sound and Vibration,* Vol. 118, No. 3, 1987, pp. 441-448.

[47]Wu, H.-Y. T., "Impact Damage of Composites," Ph.D. Dissertation, Stanford Univ., Dept. of Aeronautics and Astronautics, Stanford, CA, Dec. 1986.

[48]Olsson, R., "Theory and Experimental Verification of the Impact Response of Composite Plates," 28th Annual Technical Meeting of the Society of Engineering Science, Engineering Science Preprint 28.91022, Gainesville, FL, Nov. 6-8, 1991.

[49]Byrd, P. F., and Friedman, M. D., *Handbook of Elliptic Integrals for Engineers and Physicists,* Springer, Berlin, 1954.